RSC Advances

PAPER

View Article Online
View Journal | View Issue

Cite this: *RSC Adv.*, 2022, **12**, 9163

Ge nanowires on top of a Ge substrate for applications in anodes of Li and Na ion batteries: a first-principles study

Shaoshuai Gao, Tingyu Zhao, Dongxu Wang, Jian Huang, Youlin Xiang and Yingjian Yu *

In this study, density functional theory (DFT) was used to research the adsorption and diffusion features of Li and Na on Ge nanowires on top of a Ge substrate. The adsorption energies at different positions are 0.71–1.28 eV for Na and −2.96−−2.13 eV for Li. The adsorption energies can be further reduced by surface modification with one or two P atoms. In particular, the sidewall of the Ge nanowire modified by two P atoms is most favorable to adsorb Li/Na. In addition, we used the nudged elastic band (NEB) method to study the diffusion pathways of Li/Na on the sidewall of Ge NW and the Ge substrate and computed their energy barriers. When Li or Na diffuses across the Ge NW, the energy barrier is 0.65 or 0.79 eV, indicating that the Ge NW can be applied to anodes in lithium and sodium ion batteries. Finally, the insertion of more lithium and sodium atoms into the Ge NW would cause volume expansion and the average length of Ge–Ge bonds to increase. This work will contribute to studying the adsorption and diffusion of Li and Na on nanowires with a substrate and the volume expansion caused by the insertion of Li/Na into the nanowires. Additionally, it provides guidance for designing Ge anodes for sodium ion batteries.

Received 21st January 2022
Accepted 17th March 2022

DOI: 10.1039/d2ra00444e

rsc.li/rsc-advances

Introduction

Lithium ion batteries (LIBs) have been widely used in daily life, such as in electric vehicles (EVs), hybrid electric vehicles (HEVs), plug-in hybrid electric vehicles (PHEVs) and energy storage systems (ESSs).[1–3] However, the dramatically increasing market demand makes the availability of natural lithium resources, limited by regionality, a severe problem.[4,5] In recent years, because of the low toxicity, the natural abundance and low cost of sodium, sodium ion batteries (SIBs) have attracted researchers' interest as substitutes for LIBs.[6,7] One of the main challenges to develop SIBs is to design an anode material with good electrochemical performances.[8,9] In this regard, Ge has a relatively high reversible capacity around 350 mA h g^{-1} and retention rate that makes it a candidate for anode of SIBs.[10–16] Various theoretical and experimental works have been carried out to study the adsorption and diffusion of sodium in bulk germanium,[17], Ge thin film,[10], nanocolumnar Ge,[18], Ge nanowire[19] and phosphorus germanium alloy.[13] In particular, Ge nanowire can effectively alleviate the volume expansion caused by the metal intercalation, improve the conductivity and promote the diffusion of sodium.[20] As Ge nanowire is usually fabricated on the Ge substrate in experimental works, the effects of the substrate should not be ignored in the theoretical work.[21]

In this work, different from the previous pure Ge nanowire model, we considered the influence of the substrate on the nanowire and constructed the model including both Ge substrate and Ge NW. Next, we analyzed the behaviors of Li and Na on the Ge nanowire on top of Ge substrate. It was demonstrated that lithium and sodium tend to be adsorbed on the sidewall of Ge NW modified by two P atoms. Meanwhile, the diffusion path and energy barriers of Li/Na through Ge NW or on Ge substrate were also calculated. After more Li/Na atoms were inserted into the Ge NW, the average length of the Ge–Ge bonds increased. In this work, Ge nanowire on top of Ge substrate as anode in LIBs and SIBs is studied theoretically, which provides guidance to design anodes for SIBs.

Methods

The Ge nanowire on top of Ge substrate was investigated by generalized gradient approximation (GGA) calculations incorporated with Quantumwise Atomistix Toolkit (ATK) and the exchange–correlation function we used was Perdew–Burke–Ernzerhof (PBE).[21–29] There are 442 Ge atoms in the model and the lattice constants are $a = b = 32$ Å and $c = 55$ Å. The thickness of the vacuum layer of this model is about 36 Å. We used a 4 × 4 × 1 k-point mesh in the calculations. The structural relaxation was performed to make sure that the force on every atom

College of Physics Science and Technology, Kunming University, Kunming, Yunnan, 650214, China. E-mail: yuyingjiankmu@163.com

was less than 0.05 eV Å^{-1}. Furthermore, partial charge was calculated by Mulliken population analysis. Finally, in the NEB calculation, the force tolerance was 0.05 eV Å^{-1} and the energy convergence was less than 0.002 eV.

Results and discussion

As shown in Fig. 1(a) and (b), this model is composed of Ge substrate (blue balls) and Ge NW (purple balls). We calculated the phonon density of states (DOS) for the structure-optimized Ge nanowires on top of Ge substrates. In the negative frequency region, the DOS is zero, that is, the calculation result has no negative frequency, indicating that the system is in the state with the lowest energy, as shown in Fig. 1(c). The height and the side length of Ge NW is ~12 Å and 8 Å respectively, and the thickness of Ge substrate is ~7 Å. Considering the amount of calculation, the length of the nanowire would be extended in a follow-up research work. During the charging process of lithium/sodium ion battery, Li/Na would be adsorbed on the surface of Ge nanowire on top of Ge substrate. In order to quantitatively depict the adsorption process, the adsorption energy of Li/Na could be calculated by the following equation:

$$E_{A,M/Ge} = E_{M/G} - E_M - E_{Ge}, M = Li \text{ or } Na \quad (1)$$

where $E_{M/Ge}$ is the total energy of a Li/Na atom on the Ge model, E_M and E_{Ge} represent the energy of the alkali ion metal atom and Ge model, respectively. The adsorption energies of sodium and lithium on Ge nanowires on top of Ge substrates are presented in Fig. 2. As shown in the Fig. 2(a), the adsorption energy of Na varies from 0.71 eV to 1.28 eV. Particularly, the adsorption energies on the side wall of the NW are less than those on the top of the NW and the substrate, indicating that the special configuration would ameliorate the characteristics of Ge anode effectively.[30–33] Compared with ordinary planar Ge model, the Ge NW model in this work has a larger specific surface area. Kohandehghan *et al.*[19] experimentally demonstrated that Ge NW had higher capacity than planar germanium. Our theoretical calculation is in agreement with the experimental results. To further reduce the adsorption energy, the special Ge anode is modified by one P atom and two P atoms individually as shown in Fig. 3, which is a kind of active material. In Fig. 2, the blue bar chart shows lithium/sodium adsorption energies after modification by one P atom, and the pink bar chart shows the adsorption energies after modification by two P atoms. After Ge model is modified by two P atoms, the adsorption energies of Na on Ge nanowires change from positive to negative as shown in Fig. 2(a), indicating that the adsorption of Na on Ge model becomes stronger. Similarly, the adsorption energies of Li on Ge

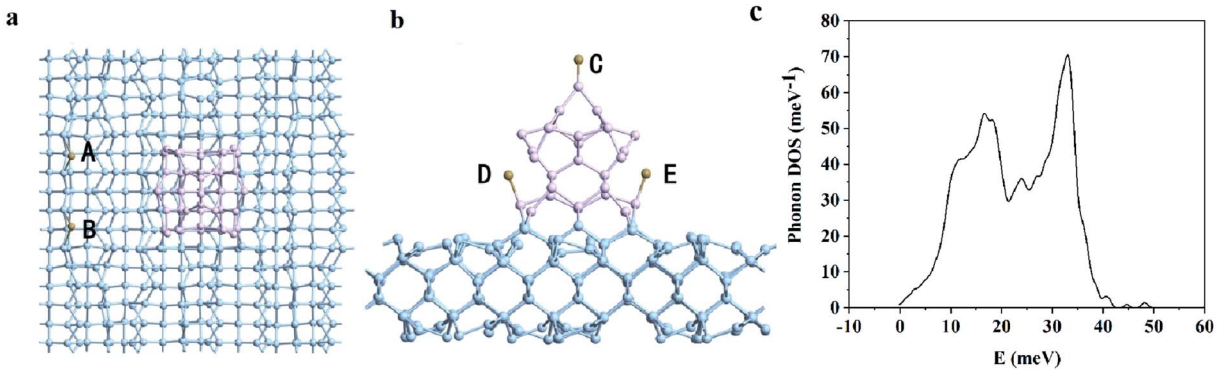

Fig. 1 (a) Top-view and (b) side-view of the atomic configuration of the Ge NW on top of substrate; (c) phonon DOS of Ge NW with substrate after structural optimization. The Ge substrate is denoted by blue balls and the Ge NW is denoted by purple balls to distinguish the two parts.

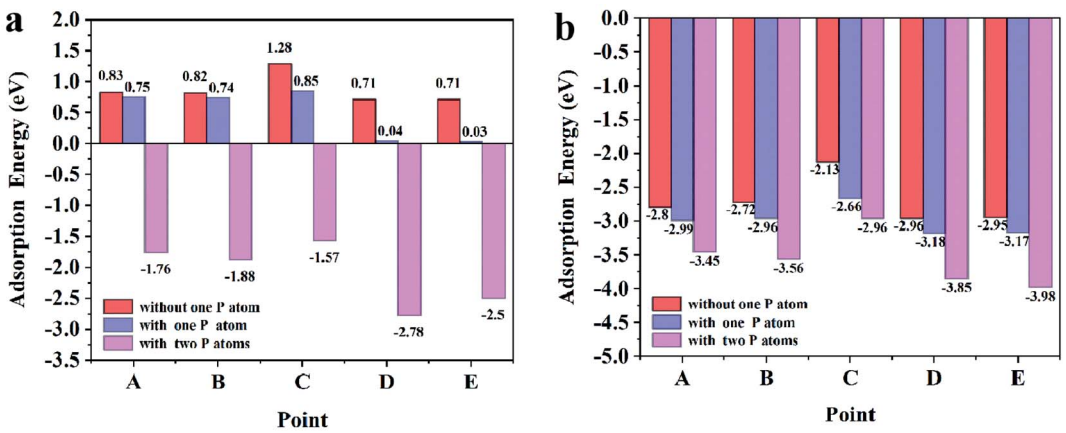

Fig. 2 (a) The adsorption energies of the sodium on the points A–E; (b) the adsorption energies of the lithium on the points A–E.

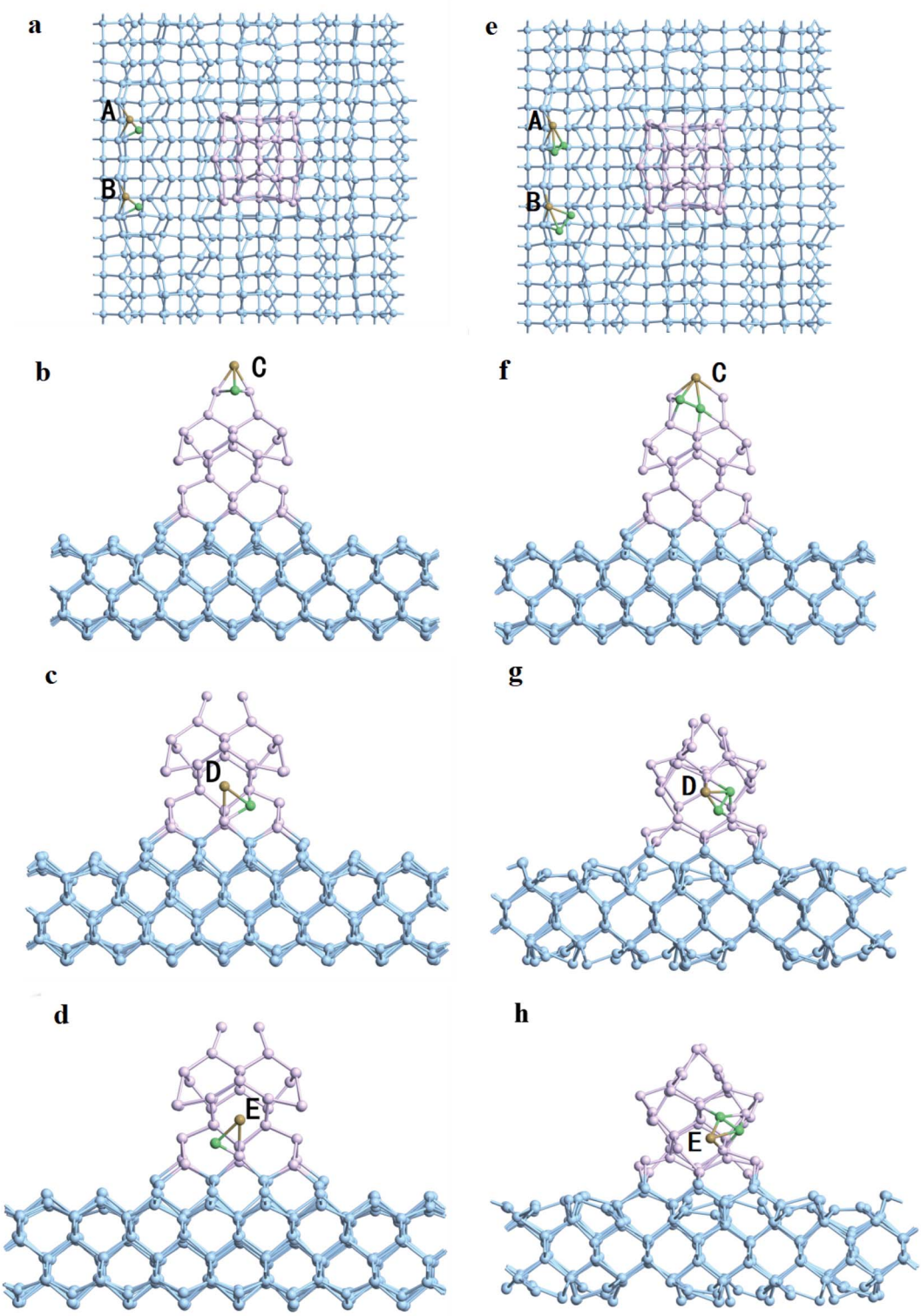

Fig. 3 Li/Na adsorbs on Ge nanowires on top of Ge substrates modified by one P atom (a–d) and two P atoms (e–h). The green ball represents P atom.

model become more negative after P decoration as seen in Fig. 2(b). According to the adsorption energies, the sidewalls of the NW modified by two P atoms are most favorable for Li and Na adsorption. It can be suggested that P modification would be beneficial for Ge anode in both Li and Na ion batteries.[34]

In order to understand the adsorption nature of Li and Na on the Ge nanowires on top of Ge substrates, the three-

dimensional charge density is shown in Fig. 4 and 5, and the partial charge was calculated by Mulliken population analysis. It can be visualized that there is electron density between Na and Ge at position *B*, evidencing the existence of Na–Ge bond. During adsorption process, Na loses 0.58*e* and two adjacent Ge atoms get 0.18*e* and 0.17*e*, as shown in Fig. 4a. After P modification, Na loses more electron to 0.62*e* while P gets 0.29*e*, as seen in Fig. 4c. Similarly, Fig. 4b and d show that in the process of bonding between Na and Ge at position *D*, Na loses 0.56*e* and Ge gets 0.19*e*. With P decoration, Na loses 0.62*e* while P gets 0.31*e*. In combination with the adsorption energy of points B and D in Fig. 2a, it can be found that Na loses more electron after the addition of P, resulting in a lower adsorption energy. For comparison, Fig. 5a–d shows the bonding and electron transfer of Li adsorbed on the Ge NW with substrate at corresponding positions. In Fig. 5a and c, Li loses 0.34*e* and Ge atoms obtain 0.16*e* and 0.17*e* respectively; after adding a P atom, Li loses more electron to 0.39*e*, and P gets 0.26*e*. Moreover, it can be found in Fig. 5b and d that Li loses 0.32*e* and Ge atoms obtain 0.12*e*; while after P modification Li loses 0.35*e* and P gets 0.31*e*. Similarly, after decoration by a P atom, the electron lost by lithium increases and the adsorption energy decreases, as shown in Fig. 2b. It can be concluded that the interaction between Na/Li and Ge nanowires becomes stronger after P modification which is in accordance with the variation of adsorption energy. Properly increasing the number of P atoms

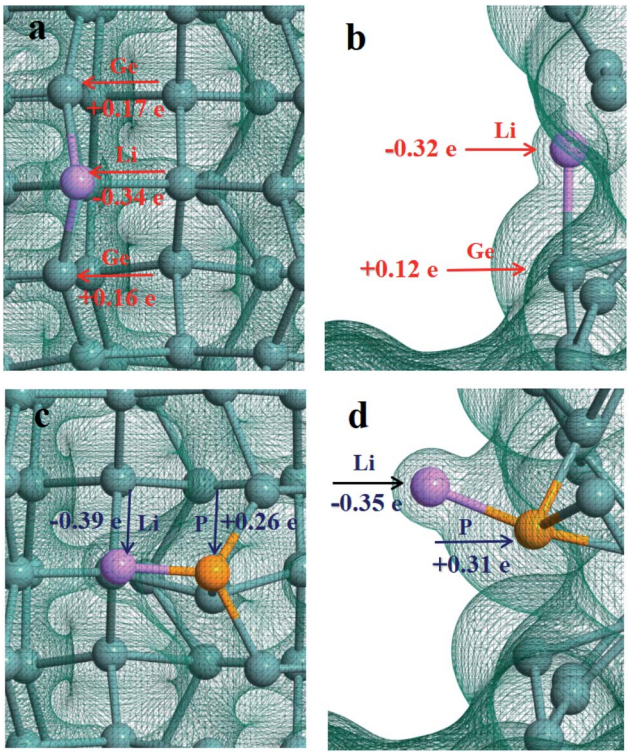

Fig. 5 Charge density of (a) Li at position *B* and (b) Li at position *D* on the Ge NW with substrate; (c) and (d) are the charge-density of Li adsorbed on Ge NW with substrate after adding a P atom. Light green, purple and yellow atoms represent Ge, Li and P, respectively.

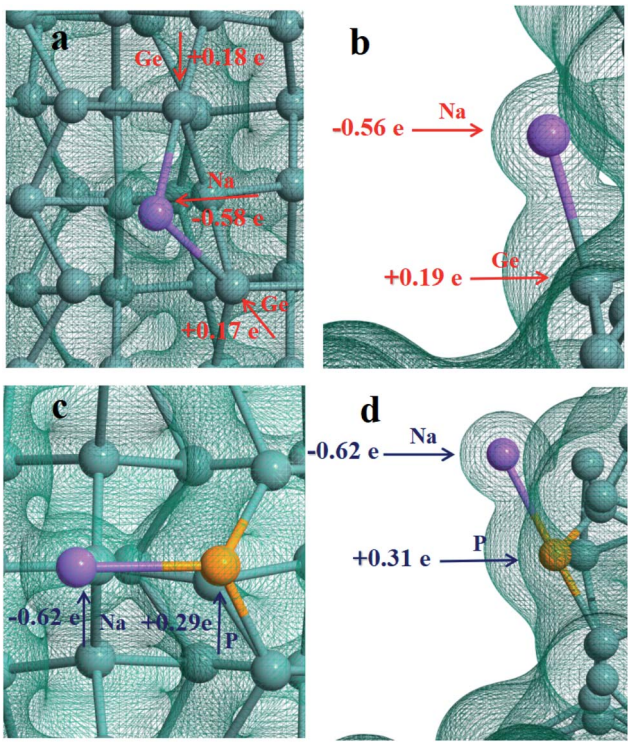

Fig. 4 Charge density of (a) Na at position *B* and (b) Na at position *D* on the Ge NW with substrate with an isovalue of 0.06 e Å^{-3}; (c) and (d) are the charge-density of Na adsorbed on Ge NW with substrate after adding a P atom. Light green, purple and yellow atoms represent Ge, Na and P, respectively.

will enhance the interaction between Li/Na and Ge nanowire on top of Ge substrate.

Furthermore, the nudged elastic band (NEB) method was used to study the diffusion pathway and the diffusion energy barriers of lithium/sodium atom on Ge model.[35,36] First, the migration of Li/Na on Ge substrate was studied. From point A to point B, the energy curve of Li/Na atom is shown in Fig. 6a and the trajectories of diffusion are visualized in Fig. 6b and c. When Li/Na migrates on the Ge substrate from A to B, the whole energy barrier is smaller than 0.44 eV/0.29 eV. Additionally, this work also investigated the diffusion of Li and Na across the Ge

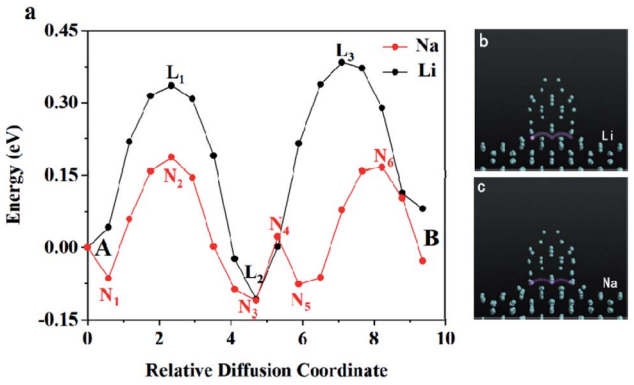

Fig. 6 (a) The energy curves for Li/Na diffusion from A to B; the side-view of the trajectories of (b) Li and (c) Na diffusion on the Ge substrate.

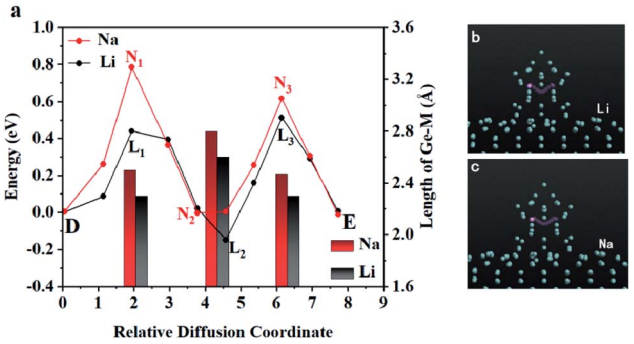

Fig. 7 (a) The energy curves along D–E pathway for the Li/Na diffusion; the side-view of the trajectories of (b) Li and (c) Na diffusion across the Ge NW. The bar chart shows the average length of Ge–M bonds on the points L_1–L_3 and N_1–N_3 (M represents Li or Na).

NW as shown in Fig. 7. In Fig. 7a, the energy barrier of Li and Na is 0.65 eV and 0.79 eV respectively, which is similar to the activation energy of the crystalline Ge (0.78 eV).[17] The diffusion coefficient (D) can be calculated by $D = D_0 \exp(-E_b/kT)$, where D_0 is the pre-exponential factor, E_b is the activation energy, k is the Boltzmann constant and T is the absolute temperature (T = 300 K here). In a certain temperature range, the diffusion coefficient increases with the improvement of the temperature.[37,38] In the migration process in Ge, the D_0 is $\sim 8.5 \times 10^{-4}$ $cm^2\ s^{-1}$ for Na and $\sim 9.1 \times 10^{-3}$ $cm^2\ s^{-1}$ for Li.[16,39,40] Thus the calculated diffusion coefficient is $\sim 4.6 \times 10^{-17}$ $cm^2\ s^{-1}$ for Na, which is completely within the scope of experimental values from 10^{-17} to 10^{-8} $cm^2\ s^{-1}$.[41] The corresponding diffusion coefficient of Li is $\sim 1.1 \times 10^{-13}$ $cm^2\ s^{-1}$, which is comparable to the experimental result ($\sim 10^{-12}$ $cm^2\ s^{-1}$).[42] The variations of the average length of the Ge–M bonds (M stands for Li or Na) in the diffusion process are exhibited by the bar chart. Obviously, the average size of the Ge–Na bonds is about 0.19 Å longer than those of the Ge–Li bonds because the radius of the sodium is larger than that of the lithium. Expectedly, both the average lengths of Ge–Li and Ge–Na bonds are inversely proportional to the energies of the system. Fig. 7b and c shows the relevant

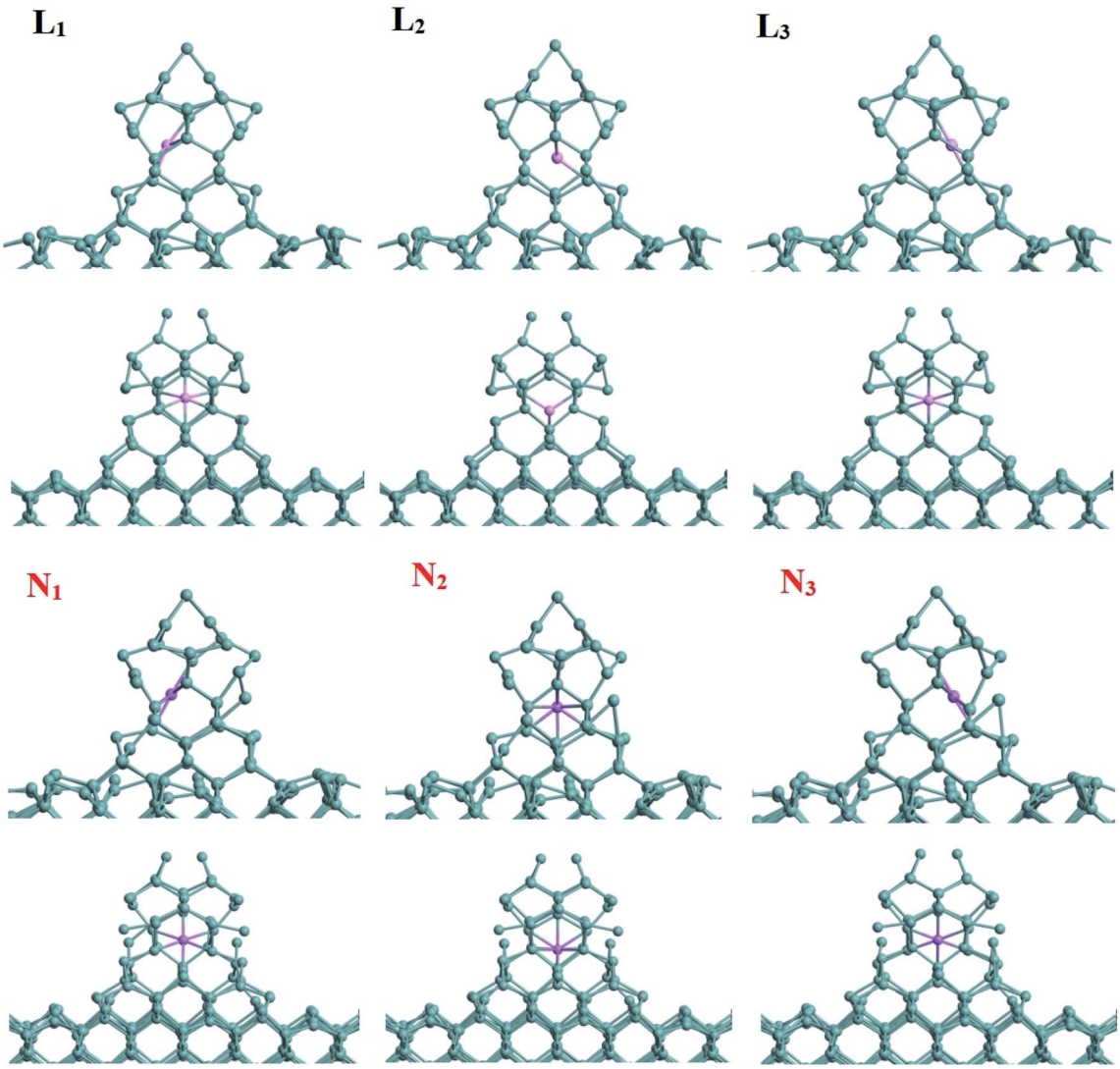

Fig. 8 The atomic configurations of the points L_1–L_3 and N_1–N_3.

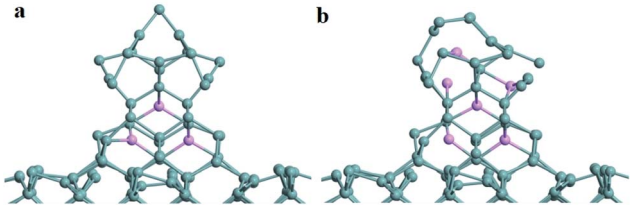

Fig. 9 (a) The relaxed structure of the Ge NW with five inserted Li atoms; (b) the relaxed structure of Ge NW with nine inserted Li atoms.

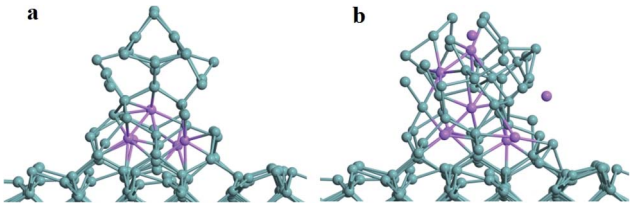

Fig. 10 (a) The relaxed structure of the Ge NW with five inserted Na atoms; (b) the relaxed structure of Ge NW with nine inserted Na atoms.

trajectories and the detailed atomic structures are shown in Fig. 8.

Besides, the Li or Na atoms inserted into the Ge nanowires on top of Ge substrates was modeled to investigate the configuration variation in the process of lithiation or sodiation process as visualized in Fig. 9 and 10. After five Li atoms are inserted into the Ge nanowires as shown in Fig. 9a, the height of the Ge nanowire decreases from 12.16 Å to 11.39 Å, while the side length of Ge NW is still around 8.68 Å without any obvious change. Meanwhile, the average length of Ge–Ge bonds changes from 2.53 Å to 2.54 Å. When nine Li atoms are inserted into Ge NW, the relaxed structure is shown in Fig. 9b. The height of Ge NW further decreases to 10.83 Å while the side length of Ge NW is almost unchanged, indicating that the Ge nanowires on top of Ge substrates would keep stable during the lithiation process without obvious volume expansion. The average length of Ge–Ge bonds is 2.56 Å.

Fig. 10a shows the relaxed atomic structure after five Na atoms are inserted into the Ge NW. The height of Ge NW reduces to 11.39 Å, while the side length increases to 9.20 Å. After five Na atoms are inserted into the Ge nanowire, some Ge–Ge bonds break and the average length of the Ge–Ge bond increases to 2.55 Å. It can be inferred that certain volume expansion of Ge NW occurs, which is consistent with the theoretical and experimental results.[16,43] After nine Na atoms are inserted in the Ge NW and relaxed as shown in Fig. 10b, two independent sodium atoms can be found. The height of Ge NW further reduces to 8.61 Å while the side length increases to 10.56 Å. Meanwhile the average length of Ge–Ge bonds increases to 2.58 Å.

Conclusions

In summary, through DFT calculations, the adsorption, diffusion and insertion of lithium and sodium on the Ge nanowires on top of Ge substrates have been theoretically studied. The results show that lithium and sodium tend to adsorb on the sidewall of Ge NW modified by two P atoms. Then, partial charge was calculated by Mulliken population analysis. We find that after P modification, Li and Na will lose more electron, resulting in a lower adsorption energy. The NEB method is used to calculate the diffusion paths and corresponding energy barriers of Li and Na on the Ge nanowires on top of Ge substrates. In addition, the insertion of sodium atoms into Ge NW would lead to certain volume expansion of the Ge NW while the Ge NW would keep stable during lithiation process. This study will contribute to research the adsorption and diffusion of lithium and sodium on nanowires with substrate and the volume expansion caused by the insertion of lithium/sodium into the nanowires. At the same time, it supplies direction for designing Ge anode in sodium ion batteries.

Author contributions

Shaoshuai Gao: writing-original draft, software, visualization; Tingyu Zhao, Dongxu Wang, and Jian Huang: software; Youlin Xiang: resources; Yingjian Yu: conceptualization, methodology, writing-original draft, writing-review & editing, supervision.

Conflicts of interest

There are no conflicts to declare.

Acknowledgements

This study was financially supported by the National Nature Science Foundation of China (Grant No. 61904073), Yunnan Fundamental Research Projects (No. 2019FGF02), Projects of Science and Technology Plans of Kunming (2019-1-C-25318000002189), Spring City Plan – Special Program for Young Talents (ZX20210014), Scientific Research Fund Project of Yunnan Provincial Department of Education (2020Y0463), and Key Laboratory of Artificial Microstructures in Yunnan Higher Education.

References

1 P. G. Anselma, P. Kollmeyer, J. Lempert, Z. Zhao, G. Belingardi and A. Emadi, *Appl. Energy*, 2021, **285**, 116440.
2 Y. Liu, Z. Huang, J. Li, M. Ye, Y. Zhang and Z. Chen, *Appl. Math. Model.*, 2021, **95**, 715–733.
3 Y. Zhang, Y. Liu, Y. Huang, Z. Chen, G. Li, W. Hao, G. Cunningham and J. Early, *Energy*, 2021, **228**, 120631.
4 Y. Yu, Y. Wang, S. Zhang, P. Zhang, S. Xue, Y. Xie, Z. Zhou, J. Li and J. Kang, *Nano Energy*, 2019, **61**, 604–610.
5 Y. Yu and S. Hu, *Chin. Chem. Lett.*, 2021, **32**, 3277–3287.
6 K. M. Abraham, *ACS Energy Lett.*, 2020, **5**, 3544–3547.
7 K. Chayambuka, G. Mulder, D. L. Danilo and P. H. L. Notten, *Adv. Energy Mater.*, 2020, **10**, 2001310.
8 T. Wang, D. Legut, Y. Fan, J. Qin, X. Li and Q. Zhang, *Nano Lett.*, 2020, **20**, 6199–6205.
9 C. Wei, S. Guo, W. Ma, S. Mei, B. Xiang and B. Gao, *Chin. J. Rare Met.*, 2021, **45**, 611–631.

10 L. Baggetto, J. K. Keum, J. F. Browning and G. M. Veith, *Electrochem. Commun.*, 2013, **34**, 41–44.
11 T. Zeng, H. He, H. Guan, R. Yuan, X. Liu and C. Zhang, *Angew. Chem., Int. Ed.*, 2021, **60**, 12103–12108.
12 J. Liu, S. Muhammad, Z. Wei, J. Zhu and X. Duan, *Nanotechnology*, 2020, **31**, 015402.
13 H. Shen, Z. Ma, B. Yang, B. Guo, Y. Lyu, P. Wang, H. Yang, Q. Li, H. Wang and Z. Liu, *J. Power Sources*, 2019, **433**, 126682.
14 K. C. Wasalathilake, N. Hu, S. Fu, J. Zheng, A. Du and C. Yan, *Appl. Surf. Sci.*, 2021, **536**, 147779.
15 K. Tseng, S. Huang, W. Chang and H. Tuan, *Chem. Mater.*, 2018, **30**, 4440–4447.
16 S. C. Jung, H. Kim, Y. Kang and Y. Han, *J. Alloys Compd.*, 2016, **688**, 158–163.
17 C. Chou, M. Lee and G. S. Hwang, *J. Phys. Chem. C*, 2015, **119**, 14843–14850.
18 P. R. Abel, Y. Lin, T. Souza, C. Chou, A. Gupta, J. B. Goodenough, G. S. Hwang, A. Heller and C. B. Mullins, *J. Phys. Chem. C*, 2013, **117**, 18885–18890.
19 A. Kohandehghan, K. Cui, M. Kupsta, J. Ding, E. M. Lotfabad, W. P. Kalisvaart and D. Mitlin, *Nano Lett.*, 2014, **14**, 5873–5882.
20 Q. Wang, C. Zhao, Y. Lu, Y. Li, Y. Zheng, Y. Qi, X. Rong, L. Jiang, X. Qi, Y. Shao, D. Pan, B. Li, Y. Hu and L. Chen, *Small*, 2017, **13**, 1701835.
21 Y. Yu, S. Hu and J. Huang, *Mater. Chem. Phys.*, 2020, **253**, 123243.
22 Y. Yu, S. Hu and J. Huang, *J. Phys. Chem. Solids*, 2021, **157**, 110226.
23 Y. Yu, S. Gao and S. Hu, *J. Alloys Compd.*, 2021, **883**, 160902.
24 S. Hu, Y. Yu, Y. Guan, Y. Li, B. Wang and M. Zhu, *Chin. Chem. Lett.*, 2020, **31**, 2839–2842.
25 Y. Yu, D. Chen, S. Gao, J. Huang, S. Hu, H. Yang and G. Jin, *RSC Adv.*, 2019, **9**, 39582–39588.
26 J. P. Perdew, K. Burke and M. Ernzerhof, *Phys. Rev. Lett.*, 1996, **77**, 3865–3868.
27 A. Kakanakova-Georgieva, G. K. Gueorguiev, S. Stafstrom, L. Hultman and E. Janzen, *Chem. Phys. Lett.*, 2006, **431**, 346–351.
28 S. A. Khan, D. Senapathi, T. Senapathi, M. S. Liao, P. Bonifassi, Z. Fan, A. K. Singh, A. Neeley, G. Hill, M. J. Huang, J. D. Watts and P. C. Ray, *Chem. Phys. Lett.*, 2011, **516**, 62–67.
29 R. B. Santos, R. Rivelino, F. B. Mota, G. K. Gueorguiev and A. Kakanakova-Georgieva, *J. Phys. D: Appl. Phys.*, 2015, **48**, 295104.
30 P. K. Nayak, L. Yang, W. Brehm and P. Adelhelm, *Angew. Chem., Int. Ed.*, 2018, **57**, 102–120.
31 M. Seo, M. Park, K. T. Lee, K. Kim, J. Kim and J. Cho, *Energy Environ. Sci.*, 2011, **4**, 425–428.
32 G. Lee, M. Sung, Y. S. Kim, B. Ju and D. Kim, *ACS Nano*, 2020, **14**, 15894–15903.
33 Y. Ko, J. Kang, G. Lee, J. Park, K. Park, Y. Jin and D. Kim, *Nanoscale*, 2011, **3**, 3371–3375.
34 Y. Sun, F. Zeng, Y. Zhu, P. Lu and D. Yang, *J. Energy Chem.*, 2021, **61**, 531–552.
35 G. Mills, H. Jonsson and G. K. Schenter, *Surf. Sci.*, 1995, **324**, 305–337.
36 S. Smidstrup, A. Pedersen, K. Stokbro and H. Jonsson, *J. Chem. Phys.*, 2014, **140**, 214106.
37 M. Schwaab and J. C. Pinto, *Chem. Eng. Sci.*, 2007, **62**, 2750–2764.
38 I. I. Fabrikant and H. Hotop, *J. Chem. Phys.*, 2008, **128**, 124308.
39 L. C. Loaiza, L. Monconduit and V. Seznec, *Small*, 2020, **16**, 1905260.
40 A. H. Sher, *J. Appl. Phys.*, 1969, **40**, 2600–2607.
41 R. Kohli and K. L. Mittal, *Developments in Surface Contamination and Cleaning: Types of Contamination and Contamination Resources*, Elsevier, 2017.
42 B. Laforge, L. Levan-Jodin, R. Salot and A. Billard, *J. Electrochem. Soc.*, 2008, **155**, A181–A188.
43 X. Lu, E. R. Adkins, Y. He, L. Zhong, L. Luo, S. X. Mao, C. Wang and B. A. Korgel, *Chem. Mater.*, 2016, **28**, 1236–1242.